

## Electrospinning of poly(lactic acid)/polyhedral oligomeric silsesquioxane nanocomposites and their potential in chondrogenic tissue regeneration

C. Gomez-Sanchez<sup>a\*</sup>, T. Kowalczyk<sup>b</sup>, G. Ruiz De Eguino<sup>c</sup>, A. Lopez-Arraiza<sup>d</sup>,  
A. Infante<sup>c</sup>, C.I. Rodriguez<sup>c</sup>, T.A. Kowalewski<sup>b</sup>, M. Sarrionandia<sup>a</sup> and J. Aurrekoetxea<sup>a</sup>

<sup>a</sup>Mechanical and Industrial Production Department, Mondragon Unibertsitatea, Loramendi, 4, 20500 Arrasate-Mondragon, Spain; <sup>b</sup>Institute of Fundamental Technological Research, Polish Academy of Sciences (IPPTAN), Pawińskiego, 5B, 02-106 Warsaw, Poland; <sup>c</sup>Stem Cell and Cell Therapy Laboratory, BioCruces, Hospital Universitario Cruces, Plaza Cruces s/n, 48903 Barakaldo, Spain; <sup>d</sup>Higher Technical School of Nautical and Marine Machines, University of the Basque Country, Maria Diaz de Haro, 68, 48920 Portugalete, Spain

(Received 24 July 2013; accepted 26 March 2014)

The study was conducted to evaluate the cytocompatibility and hydrolytic degradability of the new poly(lactic acid)/polyethylene glycol-polyhedral oligomeric silsesquioxane (peg-POSS/PLLA) nanocomposite as potential material for cartilage regeneration. PLLA scaffolds containing 0 to 5% of peg-POSS were fabricated by electrospinning. Human mesenchymal stem cells (hMSC's) were cultured *in vitro* to evaluate the cytocompatibility of the new nanocomposite material. Hydrolytic degradation studies were also carried out to analyze the mass loss rate of the nanocomposites through time. The addition of the peg-POSS to the PLLA did not affect the processability of the nanocomposite by electrospinning. It was also observed that peg-POSS did not show any relevant change in fibers morphology, concluding that it was well dispersed. However, addition of peg-POSS caused noticeable decrease in mean fiber diameter, which made the specific surface area of the scaffold to rise. hMSC's were able to attach, to proliferate, and to differentiate into chondrocytes in a similar way onto the different types of electrospun peg-POSS/PLLA and pure PLLA scaffolds, showing that the peg-POSS as nano-additive does not exhibit any cytotoxicity. The hydrolytic degradation rate of the material was lower when peg-POSS was added, showing a higher durability of the nanocomposites through time. Results demonstrate that the addition of peg-POSS to the PLLA scaffolds does not affect its cytocompatibility to obtain hyaline cartilage from hMSC's.

**Keywords:** PLLA; peg-POSS; nanocomposite; electrospinning; chondrocyte; stem cells; scaffold; cartilage repair; hydrolytic degradation

### 1. Introduction

The number of patients suffering from cartilage injury or wear is steadily growing. One of the most common disorders affecting the cartilage worldwide is osteoarthritis (OA), which has an expected exponentially increasing societal impact due to aging populations and the rising prevalence of obesity in Europe.[1] Articular cartilage is a highly specialized tissue that reduces joint friction and protects the bone ends from the shear forces associated with high mechanical load. This tissue shows a poor regenerative

---

\*Corresponding author. Email: [chgomsan@gmail.com](mailto:chgomsan@gmail.com)

capacity due to the lack of blood supply and the inability of native chondrocytes to proliferate and participate in regeneration at the injury site.[2,3]

One of the most effective methods of cartilage repair is tissue engineering approach, which involves the collaboration between medicine, biology, and engineering. Numerous studies have been carried out focusing in these subjects.[4–7] From the medical point of view, human mesenchymal stem cells (hMSC's) are a promising cell source for the engineering of cartilage tissue, due to their intrinsic capacity to differentiate to chondrocytes.[8] To improve the results in the healing of articular cartilage, as seen in Ohba's review,[9] research groups have generated articular cartilage through the *in vitro* differentiation of hMSC's on scaffolds. The whole set of hMSC's cultured into the porous polymeric scaffold is then implanted inside the body once the hMSC's have proliferated and differentiated in specific cells and new cartilage has been engineered. The scaffold needs to disappear progressively to allow new tissue regeneration. Thus, the controlled hydrolytic degradability of the material and the bioresorbability of the resulting products by the body are essential requirements of the scaffold, and require an engineering approach.[10] The engineering studies have been mainly focused on the material science since many new medicine applications have been developed due to the progress in the synthesis of new biomaterials and the discovery and modification of natural materials.[11] This modification includes the incorporation of other materials like additives or nanomolecules.[12–15] As the hydrolytic degradation rate is an important parameter which needs to be controlled, some works have analyzed the degradation through time of the material after adding various types of additives.[16–20] These studies become useful in order to introduce a material to the market with a controlled hydrolytic degradation rate. This kind of research is essential to overcome the difficulties caused by the lack of donors or the lack of patient's own material (auto-graft) that usually occur in cartilaginous diseases and other problems like patient–donor incompatibility.[21–23] Thus, the research on new biomaterials like nanocomposites [24–26] has become a new way to progress in the tissue engineering field.[27]

The PLA is a thermoplastic polymer widely used in several markets, and it is mainly characterized by its biocompatible and bioresorbable properties. It also has good strength and stiffness.[28] Three different lactides can be formed from the combination of the two optically active stereoisomeric forms (L- and D-) of the PLA: L-lactide, D-lactide, and the meso-lactide form made from a mixture of D- and L-enantiomers generally called D,L-lactide. For the production of medical polymers, L- and D,L-lactide forms are used almost exclusively,[29] being the L- form (PLLA) the most commonly used by its higher biocompatibility and degradation time.[30]

The polyhedral oligomeric silsesquioxanes (POSS) are a novel and interesting kind of nanomolecules due to their hybrid chemical composition and their 3D cage-shaped structure. The inner polyhedral structure consists of silicon and oxygen atoms surrounded by several organic groups covalently bonded to the silicon atoms. These organic groups can be modified to obtain a wide variety of polarities and reactivities.[31] Choosing properly these organic groups, POSS nanomolecules have been added via casting or melting to some commodities,[32] engineering polymers,[33,34] and high-performance polymers like polyimide (PI).[35] Up to date there are not so many applications regarding this kind of nanomolecules applied to biological purposes; POSS added to a polymer like poly(ethylene glycol)- $\alpha,\omega$ -acrylate [36] or to polyester urethane [37] are some examples. Nevertheless, the effect in the biocompatibility of the PLLA after adding poly(ethylene glycol)-POSS (peg-POSS) is unknown. Thus, a complete biological study over the hMSC's culture, proliferation, and later differentiation

into chondrogenic tissue is compulsory to check if the material is suitable for medical purposes. In the present work, apart from the nanocomposite's cytocompatibility tests, the fiber morphology after adding peg-POSS, and the effect over the electrospinning process parameters will be also studied. It is worth mentioning that, in preliminary studies carried out by our group, the addition of peg-POSS has been probed to enhance the crystallization behavior of PLLA and consequently, its mechanical properties.

This work studies the effect of the addition of different amounts of peg-POSS nanomolecules over the biological and hydrolytic degradation properties of PLLA. The aims are to check the effect of the addition of these nanomolecules over the cytocompatibility of the resulting new nanocomposite oriented to the chondrocyte culture and subsequent cartilaginous tissue growing, and to control the hydrolytic degradation rate through time of this nanocomposite. The effect of the addition of these molecules over the scaffold morphology and over the electrospinning process is studied too. To the best of our knowledge, this is the first paper about a poly(lactic acid)/polyethylene glycol-polyhedral oligomeric silsesquioxane (peg-POSS/PLLA) nanocomposite concerning biomedical applications.

## 2. Materials and methods.

### 2.1. Materials

The poly(L-lactide) used in this work (PURASORB<sup>®</sup> PL 18, PLLA), with an average molecular weight of 217.000–225.000 g/mol, was purchased from PURAC<sup>®</sup> Biomaterials (The Netherlands). The POSS nanomolecules peg-POSS, with an average molecular weight of 5576.6 g/mol, were obtained from Hybrid Plastics<sup>®</sup> (USA), and used as received. The chemical structure of the peg-POSS is shown in Figure 1. It can be highlighted that POSS nanostructures have a diameter in the range 1–3 nm.[38] The solvents N,N-dimethyl-formamide (DMF) and trichloromethane (Chloroform) used were obtained from CHEMPUR<sup>®</sup> (Poland).

The amount of peg-POSS used was 1 and 5% w/w relative to the 1 g nanocomposite. The description of the different samples prepared is shown in Table 1.

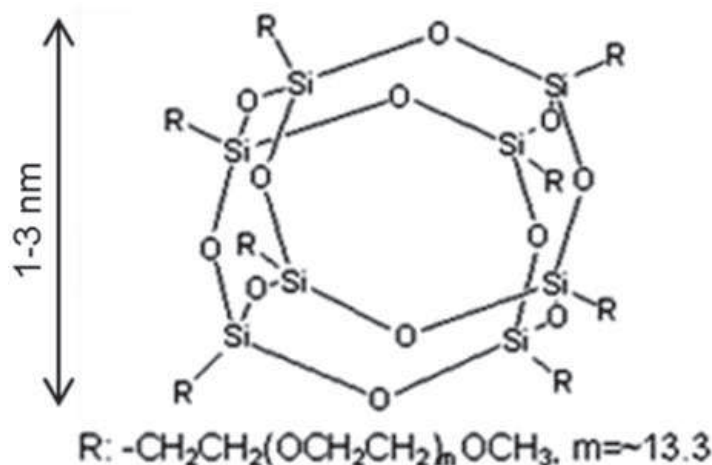


Figure 1. Chemical structure of peg-POSS.

Table 1. PLLA and peg-POSS amount of the different nanocomposites.

Denomination	Description
PLLA0	PLLA
PLLA1	+1.0% w/w peg-POSS
PLLA5	+5.0% w/w peg-POSS

## 2.2. Fabrication of peg-POSS/PLLA scaffolds by electrospinning process

The two nanocomposites were prepared by dissolving PLLA and peg-POSS in chloroform and DMF (90:10). The solution was placed in a sealed bottle and mixed in an orbital shaker for 3 h, until complete dissolution. Afterwards the solution was left overnight to ensure polymer chains disentanglement before being spun. Another solution containing PLLA only was prepared as control. The fibers were fabricated by electrospinning technique under the conditions shown in Table 2. About 0.4 ml of each solution was placed into a 1 ml plastic syringe (Brand<sup>®</sup>, Germany) and pumped by a syringe pump (New Era Pump Systems<sup>®</sup>) at a feeding rate of 0.4 ml/h. A 1 cm long blunt-end needle with an outer (inner) diameter of 0.45 mm (0.27 mm) was placed in the syringe. The equipment was setup vertically and the distance between the needle tip and the collector was adjusted to 20 cm. The randomly oriented fibers were collected in a static plate covered by a 5 cm × 12 cm aluminum foil connected to the ground as shown in Figure 2. The aluminum foil was impregnated with a surfactant to ease the remove of the fibers. A high voltage of 15 kV was applied to the system by a high-voltage regulated DC power supply (EMCO<sup>®</sup>, USA) to generate the polymer jet. The collection time was around 1 h. Finally, the aluminum foil with the fiber mat was removed from the plate and cut as 1 cm × 1 cm squares to be used for cell culture study. All the equipment was placed into a 1 m × 1 m × 1.5 m polycarbonate box to be electrically isolated from

Table 2. Selected conditions for the electrospinning process.

Parameters	Electrospinning parameters
Solvent	Chloroform 90% + DMF 10%
Feeding rate	0.4 ml/h
Distance	20 cm
Voltage	15 kV
Spinning time	1 h

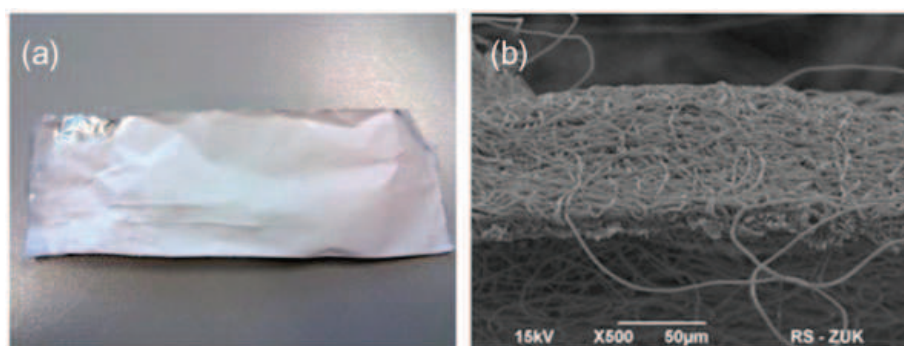


Figure 2. Electrospun peg-POSS/PLLA scaffold. (a) optical view; (b) SEM image.

outside and to avoid the environmental pollution. A solution of propan-2-ol and water (70:30) was used to disinfect the system. The experiments were carried out at room temperature (20–25 °C) and at an ambient humidity of around 45%.

### 2.3. Structural morphology of the peg-POSS/PLLA scaffolds

The morphology of the electrospun peg-POSS/PLLA scaffolds was analyzed by a scanning electron microscope (SEM, JSM-5500 LV, JEOL<sup>®</sup>, Japan). The photographs were taken under the following conditions: magnifications 500–5000, accelerating voltage 15 kV (SEM working conditions). Before the analysis, the scaffolds were coated with gold in an ion sputter coater machine (Polaron SC7620, Quorum Technologies Ltd, England) under the following conditions: argon atmosphere, current 20 mA, time 90 s. ImageJ Program (NIST, USA) was used to find the fiber diameter. For each sample three SEM images were acquired, and 33 measurements were done from each image. The measurement was done perpendicular to the fiber's axis. The pore size was calculated as follows:

Scaffold density ( $\rho_{\text{scaffold}}$ ) (1) was calculated from scaffold area and scaffold thickness (taken from SEM images).

$$\rho_{\text{scaffold}} = \text{scaffold mass} / (\text{scaffold thickness} \times \text{scaffold area}) \quad (1)$$

Scaffold porosity ( $\varepsilon$ ) (2) was calculated according to Hu et al. [39] by gravimetry from the scaffold density ( $\rho_{\text{scaffold}}$ ) and the material density ( $\rho_{\text{PLLA}} = 1.25 \text{ g/cm}^3$ ).

$$\varepsilon = 1 - (\rho_{\text{scaffold}} / \rho_{\text{PLLA}}) \quad (2)$$

Characteristic pore diameters (3) of the peg-POSS/PLLA scaffolds were calculated according to Tomadakis and Robertson [40].

$$d_{3D} = -\omega / \ln(\varepsilon) \quad (3)$$

where  $\omega$  is the average fiber diameter (calculated from ImageJ program), and  $\varepsilon$  is the scaffold porosity.

### 2.4. Viscosity measurements of the peg-POSS/PLLA nanocomposites

The viscosity of the different nanocomposites was measured through an automated falling ball micro viscometer (Anton Paar<sup>®</sup> AMVn, Germany). This device allows the determination of the dynamic viscosity of liquids with an experimental error in determining the time of ball falling below 0.002 s. The control of the temperature of the fluid is done using Peltier elements integrated in the device which allow a temperature adjustment of 0.05 °C accuracy. The measured solution was prepared solving PLLA and PLLA with different amounts of peg-POSS (1 and 5% w/w) in chloroform at room temperature. The solute concentration in the solution was 0.846% w/w for every sample. The solution was placed into a capillary and the set was automatically positioned by the machine at different inclination angles of 40°, 50°, 60°, and 70°.

### 2.5. Hydrolytic degradation studies

#### 2.5.1 Preparation of the samples

The samples for the hydrolytic degradation studies were prepared by solvent casting: PLLA and peg-POSS (0, 1 and 5% w/w relative to the 1 g nanocomposite) were

dissolved in 25 ml of chloroform at room temperature. The solution was mixed with a magnetic stirrer until completely dissolved. The different solutions were poured into Petri dishes ( $\varnothing 100$  mm), and the solvent was evaporated over 24 h at room temperature and another 24 h in a forced air heater at 35 °C, thus obtaining the peg-POSS/PLLA films without any remains of chloroform. The  $30 \times 20$  mm<sup>2</sup> samples were obtained directly from these films with a scissors.

### 2.5.2. Hydrolytic degradation procedure

The hydrolytic degradation procedure was carried out following the *ASTM F 1635-11* standard. Twenty-seven samples, 9 replicates of each nanocomposite (PLLA1 and PLLA5), and PLLA0 as control were placed individually in sealed bottles containing Dulbecco's phosphate-buffered saline physiological solution (Gibco<sup>®</sup> DPBS, Life Technologies<sup>™</sup> – Invitrogen<sup>™</sup>, USA). The physiological solution was prepared mixing DPBS and calcium chloride with double-distilled water following the manufacturer instructions. The whole set of bottles was placed into a laboratory water bath (OVAN<sup>®</sup> BATH200-12L, Spain) filled with double-distilled water at 37 °C, the human body temperature. The PBS was renewed weekly for a fresh one in order to ensure a stable pH during all the experiment. The experiment lasted 12 weeks and included 3 checkpoints: 4, 8, and 12 weeks. Every checkpoint, nine samples (three replicates of each different material) were extracted from the bath and analyzed.

### 2.5.3. Weight measurement

The samples were weighted before and after the experiments in a high-precision microbalance (OHAUS<sup>®</sup> GALAXY<sup>™</sup> 110, USA). The procedure consisted of cleaning and rinsing the extracted samples with distilled water after every checkpoint and drying them in a forced air heater at 35 °C for 72 h until the difference in weight was lower than 0.05% change in 24 h. Each sample was weighted three times, both before starting the experiment and after every checkpoint, and the average weight was calculated. The weight loss percentage was then calculated and expressed as mean  $\pm$  standard deviation (SD).

### 2.5.4. pH measurement

The pH of the physiological solution was measured weekly with a pen-type electronic pH meter (PCE-PH22<sup>®</sup>, PCE Instruments<sup>®</sup>, Spain). As the physiological fluid was renewed every week for a fresh one, the pH was measured weekly before and after the experiment. The objective was to ensure that the pH values are within the limits of the physiological range of  $7.4 \pm 0.2$  through the whole experiment.

## 2.6. Cell culture and seeding

Human bone marrow-derived mesenchymal stem cells (hMSC's) were obtained from Inbiobank Stem Cell Bank ([www.inbiobank.org](http://www.inbiobank.org)). All cells were processed at Inbiobank following manufacturing procedures under ISO9001:2000. Generated hMSC's display a typical CD13+, CD29+, CD73+, CD90+, CD105+, CD166+, CD34-, CD45-, and CD31- phenotype, and at least trilineage potential including osteocyte, chondrocyte, and adipocyte generation. hMSC's were cultured in low-glucose Dulbecco's modified

Eagle's medium (DMEM, Sigma-Aldrich<sup>®</sup>, USA) supplemented with 10% fetal bovine serum (FBS, Sigma-Aldrich<sup>®</sup>, USA) selected for MSC optimal growth. All the experiments were carried out with hMSC's having 11 or less passages. About 12 replicates (1 × 1 cm) of each material (PLLA0, PLLA1 and PLLA5) were cultured. For all experiments, hMSC's were seeded at a density of  $2 \times 10^5$  cells/scaffold on a 24-well plate, and were cultured with basal medium for 2 weeks. The medium was replaced every 2–3 days. It should be added that the scaffolds were moved to a fresh well 5 days after the seeding in order to avoid the interference with the cells that were growing on the plate surface.

For the chondrogenic differentiation, after proliferation period, hMSC's were induced to differentiate to chondrocytes by culturing them during 6 weeks with STEMPRO<sup>®</sup> Chondrogenesis Differentiation Kit (Life Technologies<sup>™</sup>, USA), following the manufacturer instructions.

### **2.7. Phase contrast and fluorescence microscopy**

Cells were analyzed under inverted microscope (Nikon<sup>®</sup>, Japan) with phase contrast lenses and photographed with a digital camera (Canon<sup>®</sup>, Japan). To visualize the nuclei of the cells, they were stained with Hoechst 33342 dye (Sigma-Aldrich<sup>®</sup>, USA) and examined under a fluorescence microscope (TE2000, Nikon<sup>®</sup>, Japan). Cartilage formation was revealed through specifically staining with alcian blue (Sigma-Aldrich<sup>®</sup>, USA). Two replicates of each material were analyzed.

### **2.8. Scanning electron microscopy**

Cells were washed in PBS, fixed in 2% glutaraldehyde in 0.1 M Sorensen's buffer (pH 7.2), washed in Sorensen's buffer with 4% sucrose, postfixed in 1% osmium tetroxide and washed in Sorensen's buffer. Samples were dehydrated through an ethanol series, immersed twice in hexamethyldisilazane before air drying and being gold coated in an ion sputter coater machine (JFC-1100, JEOL<sup>®</sup>, Japan). Images were acquired with a SEM (S-3400 N, Hitachi<sup>®</sup>, Japan). A replicate of each material was analyzed.

### **2.9. Biochemical analyses**

Sulphated-proteoglycan content in the PLLA scaffolds was measured after hydrolysis in 25 U/ml papain (Sigma-Aldrich<sup>®</sup>, USA) at 60 °C overnight with Blyscan<sup>™</sup> Glycosaminoglycan Assay (GAG, Biocolor<sup>®</sup>, UK). Six replicates of each material were analyzed at this stage: four were used for the GAG analyses, and the remaining two to obtain the microscope images.

### **2.10. Real time PCR analysis**

Total RNA was isolated from cells using High Pure RNA Isolation Kit (Roche<sup>®</sup>, Switzerland) following the manufacturer's instructions and quantified with a spectrophotometer (NanoDrop<sup>™</sup> 2000, Thermo Fisher Scientific<sup>®</sup>, USA). Real time amplification with SYBR<sup>®</sup> Green (Life Technologies<sup>™</sup>, USA) detection was performed on a 7900HT Fast Real Time PCR system (Applied Biosystems<sup>®</sup>, USA) at 95 °C for 10 min followed by 40 cycles of 95 °C for 30 s, the annealing temperature specific for each primer set, collagen type I (*COL1*) and glyceraldehyde 3-phosphate dehydrogenase

(GAPDH) at 55 °C, and collagen type II (*COL2*) at 58 °C, both for 1 min, and a final extension step of 72 °C for 1 min. Appropriate no-template controls were included in each 96-well PCR reaction, and dissociation analysis was performed at the end of every run to confirm the specificity of each reaction. Three replicates of each material were analyzed. All samples were tested in triplicate and the values of the relative amounts of the different mRNAs were calculated using the PffafI method.[41] hMSC's proliferated onto same scaffolds were used as calibrators and GAPDH gene was used as internal control.

### 3. Results

#### 3.1. Electrospinning process setup

Through the electrospinning process, very fine polymer fibers with diameters ranging from the micro- to the nano-scale can be obtained.[42] It is generally known that a highly porous microstructure with high-specific surface area gives an advantage for cell culture and growth.[43] Nanofibrous form of PLLA has an additional benefit: the constant drainage of thin nanofibrous filaments prevents from accumulation of L-lactic acid in remaining polymer. Such accumulation causes acceleration of hydrolysis of thick polyester implants caused by autocatalytic effect. At the end of the polymer degradation process, the accumulated lactic acid bursts from the remaining polymer affecting the cells growing on the scaffold. The authors have worked with a type of polyesters (aliphatic polycarbonates) that produce very weak carbonic acid during the hydrolysis and are free from autocatalytic hydrolysis.[44–47] In cartilage regeneration, an interconnected porous structure with an adequate pore size (distance between fibers) is required.[11,48,49] In the literature, many studies relating the effects of the pore size over the chondrocytic cell culture can be found. Some of them report pore size ranges such as 50–500  $\mu\text{m}$ ,[50] 100–400  $\mu\text{m}$ ,[51] 150–200  $\mu\text{m}$ ,[52] 2–465  $\mu\text{m}$ ,[53] and 10–120  $\mu\text{m}$ . [54] Although they present similar values there does not exist a general agreement, except for the minimum pore size which should obviously be larger than the cell's own size (around 5–15  $\mu\text{m}$ ). [53] In any case, in all these works where different pore size ranges were reported, the cell culture was successfully accomplished. The objective of the work is to obtain this highly porous interconnected structure made from peg-POSS/PLLA by means of the electrospinning process. Detailed process setting is required as the electrospinning process depends on the adjustment of several parameters by means of experimental trials. This search of the most stable process has been performed following the guideline of previous works conducted with some other polymer trials.[55,56] The selected parameters have been maintained for the spinning of the three materials: PLLA0, PLLA1, and PLLA5. There are some key parameters that could affect the process in a greater extent than others. They are the type and polymer concentration, the solution feeding rate, the distance between the nozzle and the target, the applied voltage, and the spinning time. There are other parameters not as significant as these ones like environmental conditions (temperature and ambient humidity), collector type, and needle type. The rest of parameters remained unchanged.

A comparison between two solvents (chloroform-DMF and trifluoroethanol) was carried out to check if the spinning of the solution was possible and to compare the solvent effect into the fibers morphology. The tests for both solvents were made under the same conditions of distance, feeding rate, and applied voltage; conditions that were subsequently analyzed in details. The electrospinning of both solutions was possible.

In Figure 3, a comparison on fiber morphology between both solvents is shown. Some differences in the fiber morphology can be observed: for the chloroform-DMF solvent (left), the fibers are not welded together, whereas in the case of the trifluoroethanol fibers are slightly welded (right). This effect was probably due to a faster evaporation of the chloroform-DMF solvent as the ejected fiber dries up before reaching the target. In the case of the trifluoroethanol, the fibers were still wet when reached the target, and welded to the previously spun fibers. A chloroform-DMF solvent was chosen as the effect of fiber bonding was not significantly pronounced.

Some of the key parameters affected directly the process regime, and their correct adjustment was significant to ensure the quality of the electrospinning process. One of the main problems consists in the electro-spray effect, which ejects polymer droplets instead of fibers to the target. Electro-spraying is directly influenced by the polymer-solvent relationship and the voltage applied. In the first case, the proper polymer-solvent content relationship was studied. Basically, phase separation of the polymeric solution should be avoided in order for the spinning process to occur, and as such, care must be taken to choose the proper polymer-solvent system. Some solvent

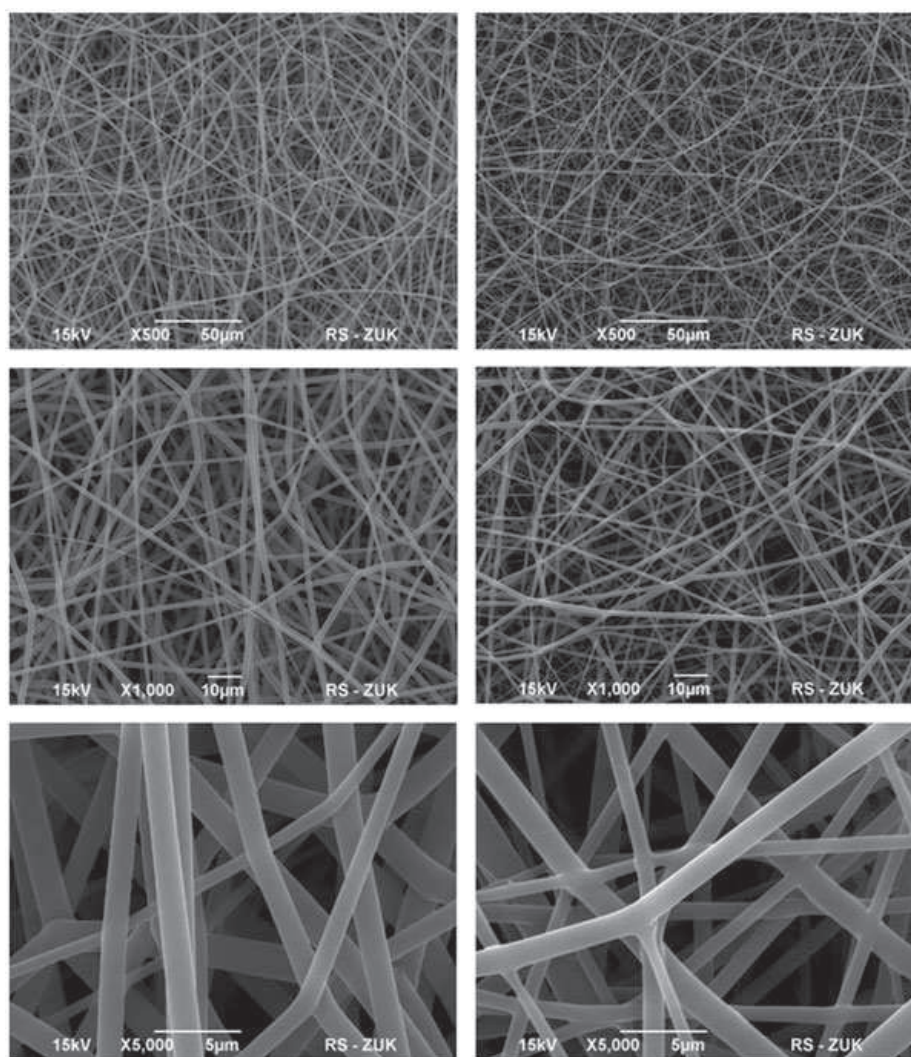


Figure 3. SEM images showing differences in fibers morphology between different solvents: chloroform-DMF (left) and trifluoroethanol (right). Photos are shown with different magnifications.

compositions were analyzed by doing some experimental trials with the electrospinning equipment and checking the resulting fibers with an optical microscope. For that purpose the solution was spun over a glass slide, placed in turn over a copper grid used as counter electrode. The solvent percentages analyzed were in the ratios 50:50 and 53:47 (both without success), 75:25 (some fibers appeared), and 90:10. Finally, this 90:10 chloroform–DMF solvent mix was used as the chosen value since a great density of fibers appeared and the difference between them, seen by means of the optical microscope, was negligible.

In the second case, once the correct solvent composition was selected, the applied voltage was also analyzed as a key parameter causing directly the electro-spray effect. The same spinning set was used in the electrospinning machine: a copper grid was used instead of an aluminum foil, with some glass slides placed on it. The samples were taken on these glass slides of 60 mm × 24 mm, during approximately 2 min. After this time, the glass slide was replaced by a new one and the voltage was increased in 2.5 kV (the voltages programmed to test in this experiment ranged from 2.5 to 30 kV). The samples were then analyzed in the optical microscope to compare the results. The minimum spinning voltage resulted in 7 kV. Below this value, electrospinning did not work and the electro-spray effect appeared. For values higher than 15 kV, some instability appeared in the jet but it did not apparently affect the fiber morphology. It does not seem to be big differences neither in the morphology nor in the amount of fibers caused by the change of voltage. An intermediate voltage of around 15 kV was chosen taking into account this equality among the results and the experience of the work performed with other polymers.[57,58]

The feeding rate represents another key parameter, since the needle tip must be fed with the proper quantity of solution before being spun to the target. A lack of material would cause an irregular and discontinuous jet to the target (also disappearance of the Taylor's cone), and an excess of material accumulated in the needle tip would lead to the possibility of this exceeding material to be thrown as big droplets to the target, consequently damaging the scaffold. In Figure 4, a comparison between two different feeding rates and the effect of a lack of material caused by insufficient feeding rate are shown. The spinning has been made with provisional values of 15 kV of applied voltage and 20 cm of distance between needle and target, and samples have been taken during 2 min and analyzed by optical microscope. It can be observed that, for the first picture, the feeding rate of 0.1 ml/h was not enough as very irregular and curly fibers were spun. Valid fibers were obtained with feeding rate values above 0.4 ml/h. For upper values there were not differences. A value of 0.4 ml/h was finally selected.

The irregular jet-like ejection represents a problem as extremely curly fibers are produced. Another cause of this effect could be due to the lack of attraction among the electrodes that depend mainly on the distance between them (between the needle tip and the target as counter-electrode) and the spinning time (directly proportional to the fiber mat thickness). According to the distance, a short one between the needle tip and the target would cause the fiber to reach the target in the unstable regime of the Taylor's cone, and a big distance would cause the disappearance of the attraction among electrodes, consequently throwing irregular fibers towards the target in both cases. An intermediate distance between electrodes must be selected. In our case, the distance was set to 20 cm. The spinning time is another key parameter that controls the proper ejection of fibers. It is limited by the maximum mat thickness that can be spun by this process and these conditions, since the polymer mat itself acts as an insulator and when a maximum thickness mat is reached the attraction among electrodes

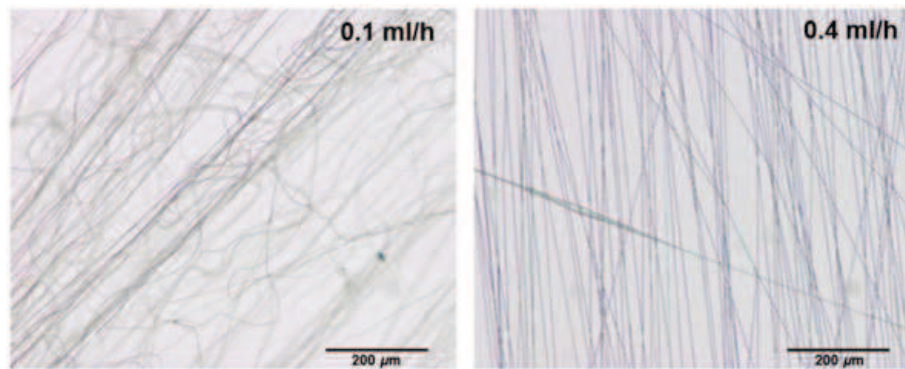


Figure 4. Optical microscope photographs showing a comparison between two different feeding rates: 0.1 ml/h, showing curly fibers (left) and the selected feeding rate of 0.4 ml/h (right). The test was carried out with a solution of PLLA with a 10% wt. of peg-POSS.

decreases and consequently the fiber reaches to the target in an irregular manner. The spinning time was set to 1 h.

### 3.2. Electrospun peg-POSS/PLLA fibrous scaffolds

In Figure 5, some SEM photographs comparing different fiber materials are shown. As a first view, a decrease in fiber diameter as the peg-POSS concentration increases can

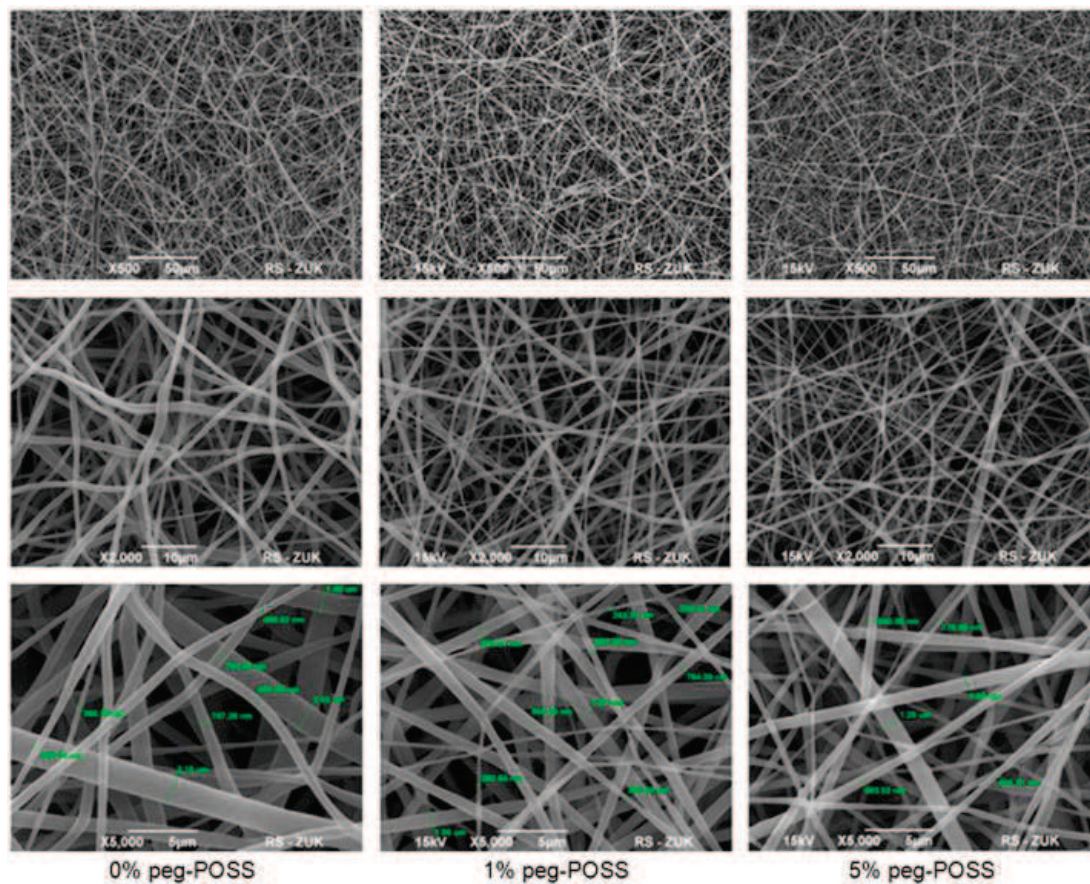


Figure 5. SEM photographs comparing the PLLA0, PLLA1, and PLLA5 samples, with different magnifications and fiber diameter measurements.

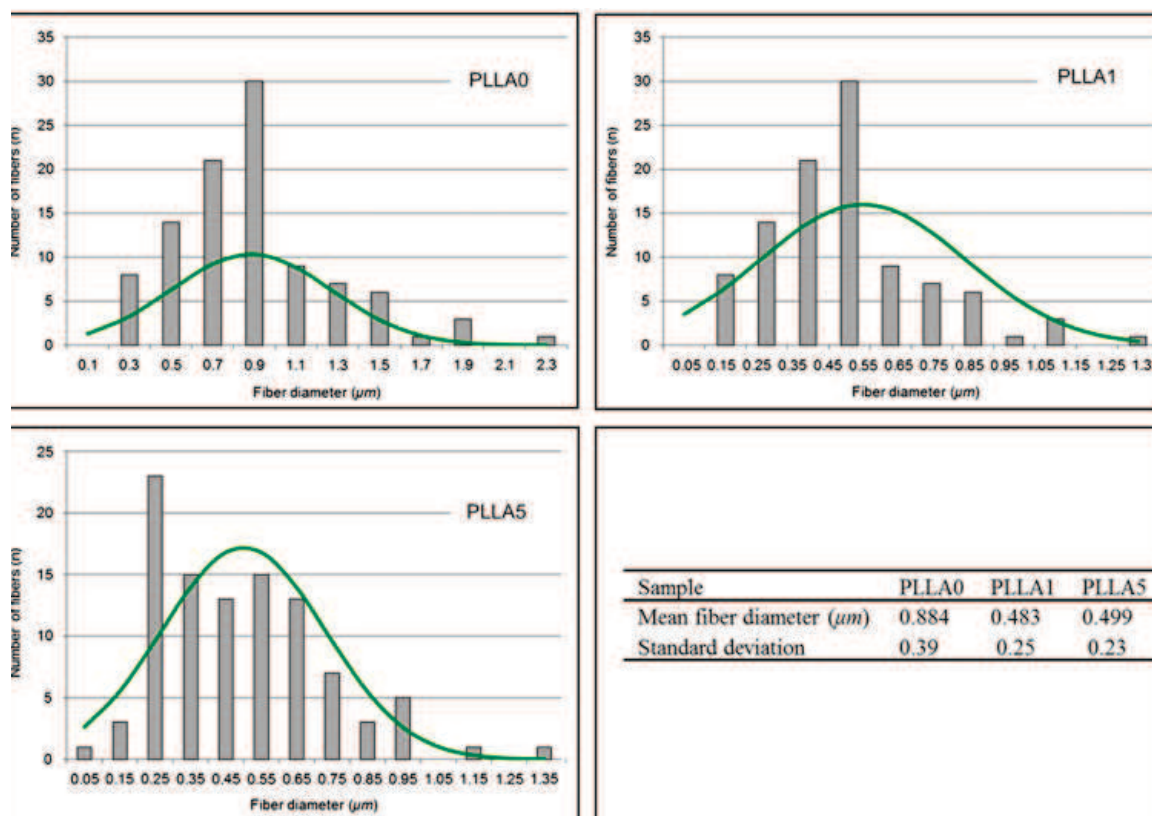


Figure 6. Statistical diagrams and results (mean fiber diameter and SD) of the PLLA0, PLLA1, and PLLA5 samples.

be observed, which is confirmed by the statistical diagrams shown in Figure 6. The results of the statistical analysis (mean fiber diameter and SD) are also displayed in Figure 6 and Table 3.

In Figure 5, it can be also seen that the scaffold is porous due to the cavity between fibers. The characteristic pore diameter and the porosity of these scaffolds are displayed in Table 3.

It was also observed in the photos that the addition of peg-POSS did not show any relevant change in fibers morphology. Since the diameter was regular along the fiber, no peg-POSS agglomeration was observed. It can be concluded that the peg-POSS is well dispersed into the fibers.

Regarding to the amount of solvent, the amount of PLLA was almost the same for the three spun samples (1 g, 0.99 g and 0.95 g for PLLA0, PLLA1, and PLLA5, respectively), so the polymer concentrations slightly changed and were around 9.20, 9.10, and 8.74% w/w, respectively. The directly proportional influence between the polymer concentration and the fiber diameter previously seen in other articles was observed.[59]

Table 3. Selected conditions for the electrospinning process.

Sample	PLLA0	PLLA1	PLLA5
Thickness ( $\mu\text{m}$ )	$45 \pm 5$	$55 \pm 5$	$52 \pm 5$
Scaffold porosity ( $\epsilon$ )	0.89	0.9	0.92
Mean fiber diameter ( $\omega$ ) ( $\mu\text{m}$ )	$0.884 \pm 0.39$	$0.483 \pm 0.25$	$0.499 \pm 0.23$
Characteristic pore diameter ( $d_{3D}$ ) ( $\mu\text{m}$ )	$7.59 \pm 3.35$	$4.58 \pm 2.37$	$5.98 \pm 2.76$

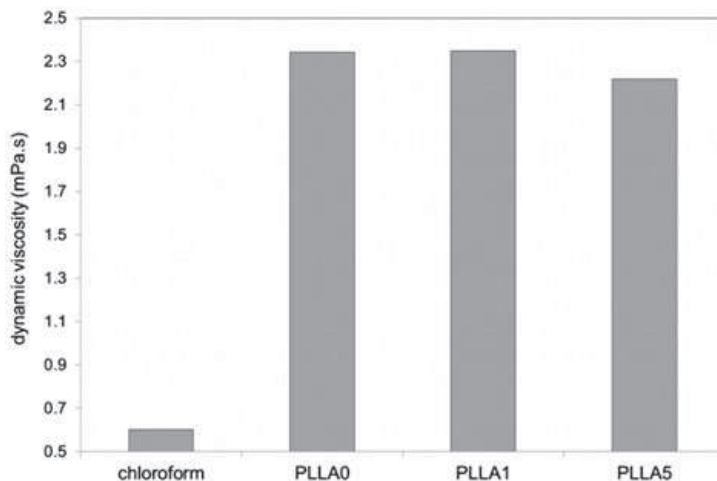


Figure 7. Dynamic viscosity values for the chloroform and the PLLA0, PLLA1, and PLLA5 samples.

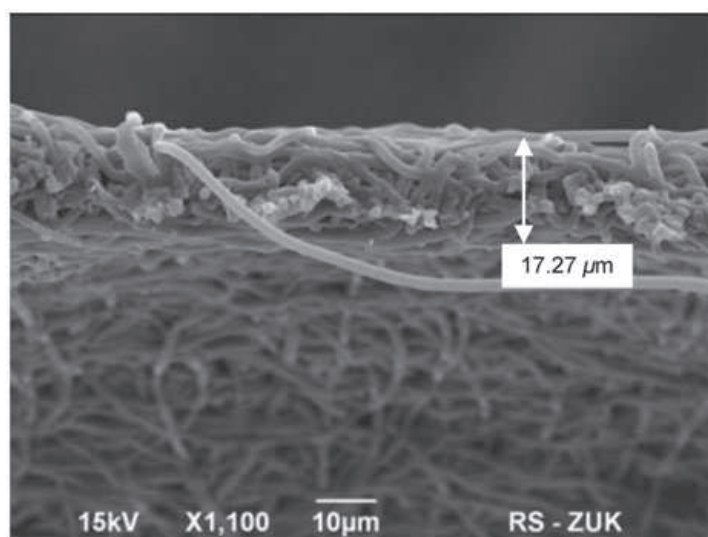


Figure 8. Thickness of the PLLA1 electrospun scaffold.

The values of the dynamic viscosity and the standard deviation for the chloroform and the three measured samples (PLLA0, PLLA1, and PLLA5) were:  $0.6017 \pm 0.0003$  mPa.s,  $2.3428 \pm 0.0019$  mPa.s,  $2.3475 \pm 0.0028$  mPa.s, and  $2.2193 \pm 0.0113$  mPa.s, respectively (Figure 7). The standard deviation values cannot be observed in the graph because they are too small in comparison with the dynamic viscosity values.

The fiber mat thickness was finally around 15–20  $\mu\text{m}$  as shown in Figure 8.

### 3.3. Hydrolytic degradation studies

The hydrolytic degradation studies displayed in Figure 9 showed that the weight loss was around the 6% for all the samples (PLLA0, PLLA1, and PLLA5) extracted after the first 4 weeks ( $6.24\% \pm 0.35$ ,  $5.4\% \pm 0.16$ , and  $6.37\% \pm 0.21$ , respectively). The

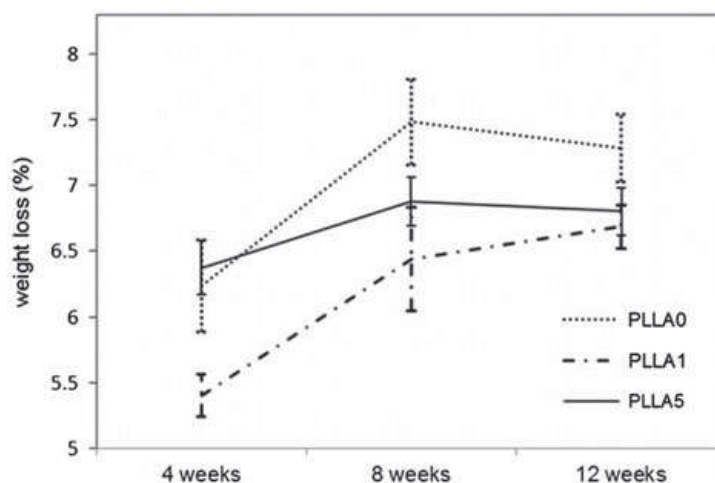


Figure 9. Weight loss percentage of the nanocomposites after the checkpoints.

weight loss of the samples extracted after 8 weeks was  $7.48\% \pm 0.33$ ,  $6.44\% \pm 0.39$ , and  $6.88\% \pm 0.19$ , respectively. The weight loss of the samples extracted after 12 weeks was  $7.29\% \pm 0.26$ ,  $6.69\% \pm 0.17$ , and  $6.8\% \pm 0.18$ , respectively. It can be seen that the maximum weight loss occurs after the first 4 weeks, probably due to a fast hydrolysis of the PLLA on the external layers of the sample. This could be even helped by an initial dissolution of the peg-POSS nanomolecules located on the surface, which are water soluble and can be considered excretable because their much lower molecular weight. After 8 weeks, the absolute weight loss rate of the samples was greater than that of the samples extracted after the first 4 weeks; but was not as greater for the relative weight loss, as the difference between these two checkpoints was around the 1%. In the final checkpoint of the experiment (12 weeks), the absolute weight loss percentage was the biggest for the PLLA1 sample, but not for the other two samples, whose values were similar or slightly lower than those of the samples extracted after 8 weeks. The relative weight loss percentage of the samples extracted after 12 weeks was bigger than that of the extracted after 4 weeks ones.

In Figure 9, it can be seen that the weight loss after the first 4 weeks tends to stabilize. This behavior could be related to the fact that, when samples were extracted from the fluid, they presented a kind of skin over the surface, probably due to the deposition of PBS salts and debris of hydrolytically degraded polymer and peg-POSS. This skin could obstruct the hydrolysis process and the exchange of polymer at the sample–fluid interface. A similar effect was found to happen in poly-D-L-lactide/nano-hydroxyapatite nanocomposites.[16] The weight loss of the PLLA1 and PLLA5 samples was lower for every checkpoint than that of the PLLA0, indicating an increased durability of the nanocomposites. The peg-POSS seemed to delay the hydrolytic degradation of the PLLA. On the other hand, the weight loss of the PLLA1 sample is lower than that of PLLA5, indicating a possible saturation of the polymer.

The pH remained within the limits ( $7.4 \pm 0.2$ ) during all the experiment. Nevertheless, a small decrease in the pH values was observed weekly as the samples became degraded: the pH of the fresh PBS was around 0.2 higher than the pH of the final PBS containing debris of hydrolytically degraded polymer and peg-POSS. This effect was reported to happen due to the release of lactic acid.[60]

### 3.4. Cell morphological studies

hMSC's were cultured onto electrospun peg-POSS/PLLA scaffolds for 2 weeks. After that period, cells were stained with Hoechst dye to study their viability and attachment capacities. Figure 10 displays the stained nuclei of hMSC's onto PLLA0, PLLA1, and PLLA5.

These pictures evidence that hMSC's were able to attach and to spread onto the three different electrospun peg-POSS/PLLA and pure PLLA scaffolds. It was also observed that the addition of peg-POSS nanomolecules has not decreased the cell viability.

hMSC's are adult stem cells capable to differentiate into cartilaginous lineage. To complete an optimal chondrogenic process, it is very critical to get an appropriate cellular confluence. SEM studies were performed to confirm whether hMSC's reached optimal confluence for their differentiation into chondrocytes.

hMSC's cultured for 2 weeks onto three different scaffolds (Figure 11(a)–(c)) formed a continuous sheet, with similar appearance under scanning electron microscopy. The detail (Figure 11(d)) shows the sheet formed on the fibers containing 1% w/w of POSS. These results predict a high-quality subsequent chondrogenesis process.

The extracellular matrix (ECM) rich in glycosaminoglycans (GAG) deposition is a characteristic of mature functional chondrocytes.[61] Cartilage is 15–25% GAG dry weight.[62] Proteoglycans make up ECM of articular cartilage and contribute to its mechanical properties.[61,63] hMSC's were induced to undergo chondrogenesis for 6 weeks and after that, each scaffold was stained with alcian blue which specifically stains GAG.[64]

Figure 12 shows the aggregates of cartilage containing blue GAG stained on three different scaffolds. These results demonstrate the presence of GAG in all electrospun peg-POSS/PLLA scaffolds.

In order to compare the ability of hMSC's induced differentiation onto electrospun peg-POSS/PLLA scaffolds to produce GAG, the amount of GAG generated was measured in each scaffold. All the scaffolds exhibited a high degree of GAG production. Moreover, the degree of GAG secretion was similar for all of them. As depicted in Figure 13, no significant differences in GAG content were observed between the three types of electrospun scaffolds. These results indicated that the competency to secrete GAG of chondrocytes derived from hMSC's was not affected. Even this competency to secrete GAG slightly increased comparing the samples containing peg-POSS (PLLA1 and PLLA5) to that not containing (PLLA0). It can be concluded that peg-POSS does not inhibit the secretion of GAG.



Figure 10. Hoechst stained hMSC's onto electrospun peg-POSS/PLLA scaffolds after cell spreading. (a) PLLA0, (b) PLLA1, and (c) PLLA5.

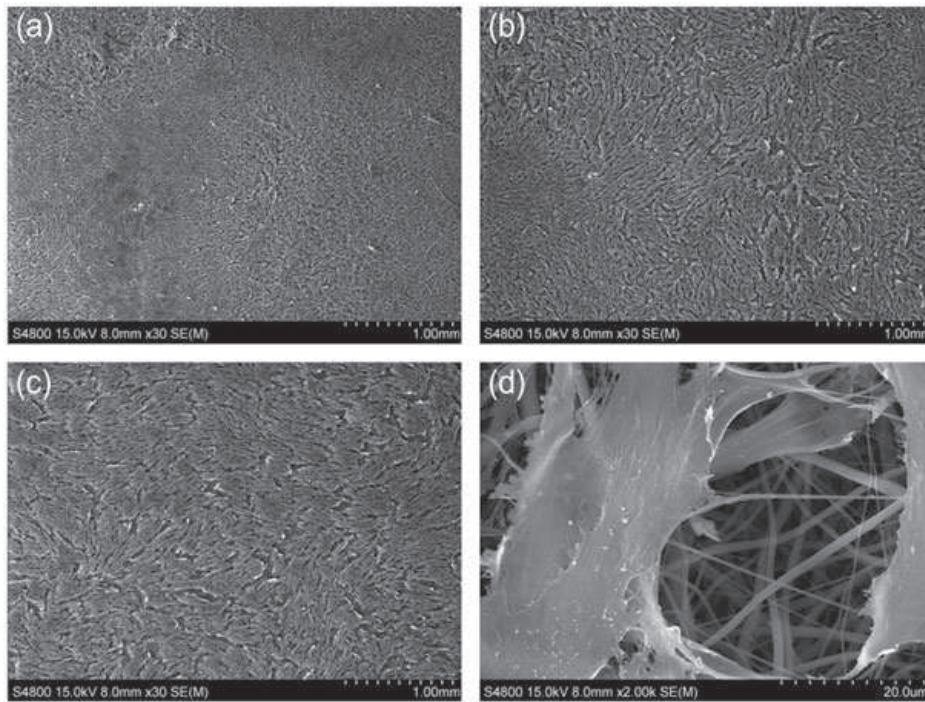


Figure 11. SEM photomicrographs showing sheet formation by hMSC's cultured on electrospun peg-POSS/PLLA scaffolds for 2 weeks. (a) PLLA0, (b) PLLA1, (c) PLLA5, and (d) detail of hMSC's on PLLA1.

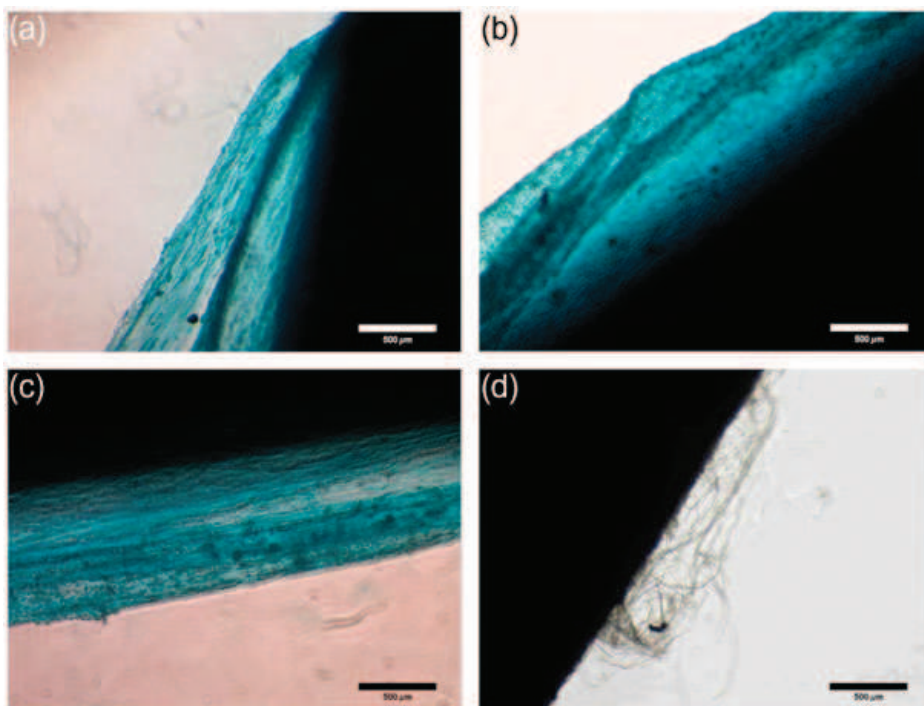


Figure 12. Aggregates of cartilage containing blue GAG stained onto electrospun peg-POSS/PLLA scaffolds. (a) PLLA0, (b) PLLA1, (c) PLLA5, and (d) PLLA0 without cells as negative control.

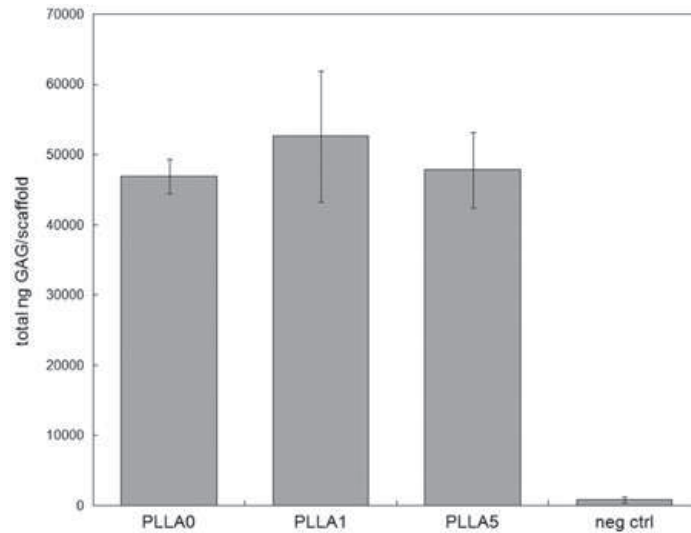


Figure 13. Quantification of GAG in hMSC-derived cartilage onto electrospun peg-POSS/PLLA scaffolds. Neg ctrl: negative control (scaffold without cells). Data are presented as mean  $\pm$  SD.

Collagen type II (*COL2*) is the typical marker of differentiated chondrocytes in hyaline cartilage, as opposed to collagen type I (*COL1*), which is expressed by dedifferentiated chondrocytes as well as in fibrocartilage. The articular cartilage contains 95% of type II collagen fibers which makes up 50% of the cartilage dry weight. This network provides tensile strength to the tissue.[62,65] Real-time PCR study was used to analyze the mRNA expression of articular cartilage-specific genes from hMSC's-differentiated chondrocytes normalizing to that of hMSC's.[66–68]

The expression of *COL2* and *COL1* genes in hMSC-derived chondrocytes showed some differences between the three types of scaffolds. The relative expression of *COL2* gene in every scaffold was greatly increased in hMSC-derived chondrocytes compared to hMSC's ( $144.58 \pm 44.06$ ,  $136.81 \pm 33.61$ , and  $204.17 \pm 39.91$ , respectively), whereas *COL1* gene expression slightly increased ( $0.73 \pm 0.08$ ,  $1.33 \pm 0.35$ , and  $1.87 \pm 0.45$ ) (Figure 14). The strong increase in the fold expression of *COL2* gene in the cells

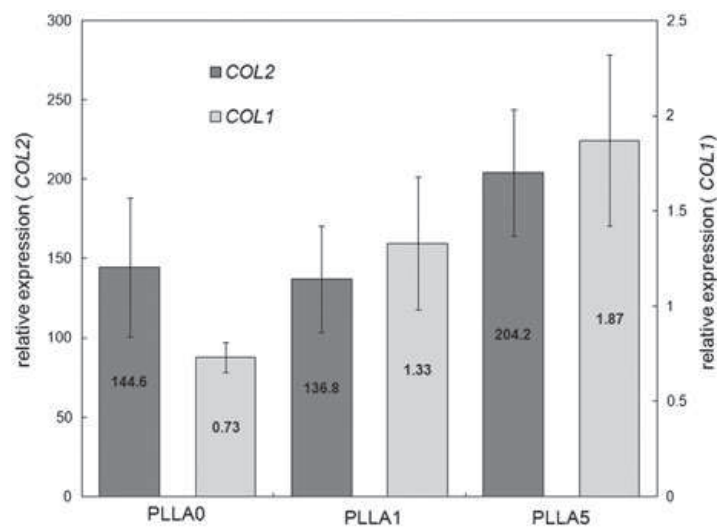


Figure 14. Relative gene expression of articular cartilage markers (*COL1* and *COL2*) in hMSC-derived chondrocytes cultured onto electrospun peg-POSS/PLLA scaffolds. The mRNA values of each gene were normalized to GAPDH. Data are presented as mean  $\pm$  SD.

seeded on the different scaffolds compared to undifferentiated hMSC's (more than 100-fold increase) demonstrates that the chondrogenesis process was induced properly. Moreover, PLLA5 induced the expression of *COL2* to a greater extent when comparing to PLLA0 and PLLA1. In contrast, the level of induction of *COL1* gene was very slight, and the differences between the scaffolds were neither relevant nor comparable to those observed in *COL2* gene expression. For all the scaffolds, the high levels of *COL2* gene expression compared to *COL1* suggest a proper cartilage differentiation process. Furthermore, the increased ratio of expression *COL2* to *COL1* implies a progress toward mature cartilage phenotype in hMSC-derived chondrocytes as seen elsewhere.[69,70]

These results suggest that the addition of peg-POSS to PLLA scaffolds did not decrease the ability of hMSC's to differentiate to chondrocytes onto scaffolds.

#### 4. Discussion

The present work studies the effect of the addition of the peg-POSS nanomolecules in various amounts over the manufacturing process and over the cytocompatibility and the morphology of some electrospinning-made PLLA scaffolds. The hydrolytic degradation behavior of the material is studied too.

Morphological studies confirm that the peg-POSS does not change the fiber shape. It seems that the peg-POSS is well dispersed into the fibers. However, a noticeable decrease in mean fiber diameter can be observed as peg-POSS concentration increases. This effect could be explained due to the viscosity of the solvent–nanocomposite solution, which is identified as the dominant variable that determines the fiber diameter.[71] In our study, the solution viscosity decreases as the content of peg-POSS increases. It is known that the diameter of electrospun fibers decreases with decreasing solution viscosity,[72] therefore, the reduction of the fiber diameter as peg-POSS content increases could be explained. This effect could be also explained regarding to the polymer/solvent ratio: the directly proportional influence between the polymer (referring only to PLLA) concentration and the fiber diameter previously seen in other articles was observed,[42,59] as fiber diameter decreased in the same manner as polymer concentration did. The decrease in fiber diameter also has the effect of increasing the specific surface area of the scaffold, which has been reported to enhance the cell culture.[73] The addition of peg-POSS neither had any detrimental effect on the processing method since any major change was observed on the electrospinning parameters of the peg-POSS/PLLA regarding to those of the pure PLLA. The maximum thickness of scaffold which could be manufactured by electrospinning, due to the lack of attraction between the needle and the static collector, remained unchanged for all the scaffolds. However, the use of rotary drum collector would enable to construct thicker scaffolds (up to 250  $\mu\text{m}$ ).

The hydrolytic degradation rate or weight loss percentage of the material was lower when peg-POSS was added, showing a higher durability of the nanocomposites. On the other hand, after an initial mass loss, the hydrolytic degradation rate tended to stabilize through time. An explanation of these effects would lead to the analysis of the hydrolytic degradation mechanisms reported in the literature. Grizzi et al. [60] investigated the hydrolytic degradation behavior of some aliphatic polyesters such PLLA, and they suggested the existence of two phenomena that could affect the degradation. (1) An autocatalytic effect on the ester hydrolysis of the polymer caused by the increased number of carboxylic chain ends. (2) A diffusion or leaching (from the inner to the outer

part of the material) of the oligomers dissolved in the aqueous medium. Taking into account both phenomena, they also suggested two degradation behaviors based on the thickness of the samples. (a) for large thickness samples, the initial dissolution and diffusion to the aqueous medium of the oligomers located on the outer part (surface), and the difficulties in the diffusion of the residual lactide and oligomers located on the inner part, would lead to an heterogeneous degradation between the inner/outer part of the sample. The oligomers and residual lactide degraded on the inner part would not be able to be leached as fast as those located on the surface, and they would cumulate giving rise to the previously reported autocatalytic effect for the hydrolysis. This would accelerate the degradation process of the inner part of the sample regarding to the surface, and would cause the formation of a skin composed of less degraded polymer. (b) for small thickness samples such casting made films (<1 mm), it would not exist the heterogeneous degradation mechanism. The oligomers and residual lactide degraded within the material should be able to be leached as soon as they become soluble, so the autocatalytic effect would not take place, and the material would degrade more slowly.

Our degradation data agree with the behavior reported by Grizzi et al. [60]. For films, there is an initial mass loss, caused by the water swelling and the initial dissolution and rapid diffusion of the oligomers and the peg-POSS. Over the next few weeks the hydrolytic degradation tends to stabilize, mainly because the nonexistence (or weak) autocatalytic effect. According to the nanocomposites, the peg-POSS nanomolecules could contribute to the increase of hydrophilicity of the PLLA (considered hydrophobic), [74] thus enhancing the diffusion of the oligomers and slowing the degradation, as our degradation data show. Yang et al. reported a similar effect for the  $\alpha$ -TCP/PLGA nanocomposites. [75] They also suggested the buffering of the acidic end groups of the oligomers and the subsequent neutralization of the environment through the use of  $\alpha$ -TCP nanoparticles, in which the use of peg-POSS nanomolecules could have impact too. It seems that peg-POSS slows the hydrolytic degradation rate of PLLA films, but further studies up to the complete degradation of the material would be needed to better understand its behavior and the effect of these nanomolecules.

The biological studies show that hMSC's were able to attach and to spread in a similar way onto the different types of electrospun peg-POSS/PLLA and pure PLLA scaffolds. It was observed that the addition of peg-POSS nanomolecules neither decreased the cell viability nor their capacity to form a monolayer. SEM studies were performed to confirm whether hMSC's reached optimal confluence for their differentiation into chondrocytes. The results predicted a high-quality subsequent chondrogenesis process. Results also demonstrate a competence of hMSC's to differentiate into chondrocytes onto all the scaffolds. The hMSC-differentiated chondrocytes were able to secrete GAG efficiently, a specific characteristic of mature chondrocytes. In order to compare the ability of hMSC's-induced differentiation onto electrospun peg-POSS/PLLA scaffolds to produce GAG, the amount of GAG generated was measured in each scaffold. All the scaffolds exhibited a high degree of GAG production, being their GAG secretion level similar for all of them. These results indicated that the competency to secrete GAG of chondrocytes derived from hMSC's was not affected by the addition of peg-POSS. Even this competency to secrete GAG slightly increased comparing the samples containing peg-POSS (PLLA1 and PLLA5) to that not containing (PLLA0). It can be concluded that peg-POSS does not inhibit the secretion of GAG. The hMSC-derived cartilage showed high levels of *COL2* compared to *COL1* gene expression for all the scaffolds, suggesting a proper cartilage differentiation process. There were slight

differences between the three different types of peg-POSS/PLLA and pure PLLA scaffolds in the induction of *COL1* gene expression. However, there was an important increment in *COL2* gene expression, indicating that peg-POSS/PLLA does not alter significantly the expression of chondrogenesis markers. The addition of peg-POSS to PLLA scaffolds did not affect its cytocompatibility to obtain hyaline cartilage from hMSCs. In addition, the pH remained stable within the physiological limits during all the hydrolytic degradation experiment, so the cell culture would not be affected.

On the other hand, it is worth mentioning that, according to the results, even having our scaffolds a smaller pore size range than the range reported in the literature, the hMSC's were able to undergo a proper chondrogenic differentiation, as it is shown by the presence of GAG and the increasing expression of cartilage specific genes (*COL2* and *COL1*), thus demonstrating that a proper cell culture could be possible at lower pore sizes. This could be explained by the fact that electrospun fiber mats behave differently from rigid porous materials. It was demonstrated that electrospun mats can be infiltrated by cells for fiber diameters as low as 0.22  $\mu\text{m}$  and average pore diameter only 1.5  $\mu\text{m}$ .<sup>[76]</sup> This pore size is much smaller than the minimum pore size for cell infiltration previously reported (around 5–15  $\mu\text{m}$ ). This behavior is explained by the ability of cells to push individual fibers in electrospun mats. In addition, for fibers thinner than 1  $\mu\text{m}$ , the cell proliferation increases with decreasing fiber diameter.<sup>[77]</sup> This effect is attributed to very high specific surface area that causes protein absorption from cell medium. The surface of nanofibers covered with proteins enhances cell attachment and proliferation.<sup>[73]</sup> The best results for cells growth on electrospun mats are porosities 70–95% and pore size 5–50  $\mu\text{m}$ .<sup>[76,77]</sup> The calculated average pore size is within the optimal range for cells attachment. Very high porosity of the scaffold allows the cells to infiltrate the structure by pushing aside the nanofibers to create the space necessary for attachment and proliferation. As can be seen from SEM micrographs (Figure 5), the increased content of peg-POSS increases the presence of thin fibers. Their large specific surface area enhances cells attachment and proliferation. This effect is not so strongly pronounced when taking into consideration only the mean fiber size (Figure 6), but is clearly visible on histogram (Figure 6) (fibers of size ca. 0.25  $\mu\text{m}$  consist of 23% of total number of fibers). Thus, the increase in specific surface area by the decrease of the fiber diameter previously mentioned could explain the enhancement in the chondrocytic cell culture.

As conclusions, the results show that the biological properties of PLLA were not deprived after adding peg-POSS. It seems that the peg-POSS does not present any nanotoxicity. The results did not show any relevant change either in the manufacturing process or in the fiber morphology after adding peg-POSS, except for the decrease in mean fiber diameter. On the other hand, it seems that peg-POSS slows the hydrolytic degradation rate of PLLA films. Taking into consideration these points, it may be suggested the peg-POSS/PLLA nanocomposite as a new material to obtain suitable scaffolds for the regenerative medicine.

### Acknowledgements

The authors wish to thank Mr Ryszard Strzałkowski (IMDiK PAN and IPPT PAN, Poland) for his excellent evaluation of SEM images and David Alonso de Mezquía (Mondragon Unibertsitatea, Spain) for his invaluable assistance with the viscosity measurements.

## Funding

This work was supported by the Provincial Council of Gipuzkoa through the DICELL project (expedient 64/08), by the Basque Government through the project IE10-272, and by the Spanish Education and Science Ministry through the project PSE-010000-2009-3. C. Gomez-Sanchez stay at IPPT PAN was partially supported by Polish Ministry of Science Grant No. N508 031 31/1740.

## References

- [1] Coleman CM, Curtin C, Barry FP, O'Flatharta C, Murphy JM. Mesenchymal stem cells and osteoarthritis: remedy or accomplice? *Hum. Gene. Ther.* 2010;21:1239–1250.
- [2] Tae SK, Lee SH, Park JS, Im GI. Mesenchymal stem cells for tissue engineering and regenerative medicine. *Biomed. Mater.* 2006;1:63–71.
- [3] Chen G, Liu D, Tadokoro M, Hirochika R, Ohgushi H, Tanaka J, Tateishi T. Chondrogenic differentiation of human mesenchymal stem cells cultured in a cobweb-like biodegradable scaffold. *Biochem. Biophys. Res. Commun.* 2004;322:50–55.
- [4] Maienschein J. Regenerative medicine's historical roots in regeneration, transplantation, and translation. *Dev. Biol.* 2011;358:278–284.
- [5] Vacanti J. Tissue engineering and regenerative medicine: from first principles to state of the art. *J. Pediatr. Surg.* 2010;45:291–294.
- [6] Atala A. Regenerative medicine strategies. *J. Pediatr. Surg.* 2012;47:17–28.
- [7] Polak DJM. Regenerative medicine: a primer for paediatricians. *Early Hum. Dev.* 2009;85:685–689.
- [8] Dominici M, Le Blanc K, Mueller I, Slaper-Cortenbach I, Marini F, Krause D, Deans R, Keating A, Prockop DJ, Horwitz E. Minimal criteria for defining multipotent mesenchymal stromal cells. The International Society for Cellular Therapy position statement. *Cytotherapy.* 2006;8:315–317.
- [9] Ohba S, Yano F, Chung U. Tissue engineering of bone and cartilage. *IBMS BoneKEy.* 2009;6:405–419.
- [10] Liu C, Xia Z, Czernuszka J. Design and development of three-dimensional scaffolds for tissue engineering. *Chem. Eng. Res. Des.* 2007;85:1051–1064.
- [11] Hutmacher DW. Scaffolds in tissue engineering bone and cartilage. *Biomaterials.* 2000;21:2529–2543.
- [12] Armentano I, Dottori M, Fortunati E, Mattioli S, Kenny JM. Biodegradable polymer matrix nanocomposites for tissue engineering: a review. *Polym. Degrad. Stab.* 2010;95:2126–2146.
- [13] Pan H, Qiu Z. Biodegradable poly(L-lactide)/polyhedral oligomeric silsesquioxanes nanocomposites: enhanced crystallization, mechanical properties, and hydrolytic degradation. *Macromolecules.* 2010;43:1499–1506.
- [14] Ray S, Maiti P, Okamoto M, Yamada K, Ueda K. New polylactide/layered silicate nanocomposites. 1. Preparation, characterization, and properties. *Macromolecules.* 2002;35:3104–3110.
- [15] Chang J, An Y, Sur G. Poly(lactic acid) nanocomposites with various organoclays. I. Thermomechanical properties, morphology, and gas permeability. *J. Polym. Sci., Part B: Polym. Phys.* 2003;41:94–103.
- [16] Chen L, Tang CY, Tsui CP, Chen DZ. Mechanical properties and *in vitro* evaluation of bioactivity and degradation of dexamethasone-releasing poly-D-L-lactide/nano-hydroxyapatite composite scaffolds. *J. Mech. Behav. Biomed. Mater.* 2013;22:41–50.
- [17] Nieddu E, Mazzucco L, Gentile P, Benko T, Balbo V, Mandrile R, Ciardelli G. Preparation and biodegradation of clay composites of PLA. *React. Funct. Polym.* 2009;69:371–379.
- [18] Cheung HY, Lau KT, Pow YF, Zhao YQ, Hui D. Biodegradation of a silkworm silk/PLA composite. *Composites Part B.* 2010;41:223–228.
- [19] Lee YH, Lee JH, An IG, Kim C, Lee DS, Lee YK, Nam JD. Electrospun dual-porosity structure and biodegradation morphology of Montmorillonite reinforced PLLA nanocomposite scaffolds. *Biomaterials.* 2005;26:3165–3172.
- [20] Gaona LA, Gómez Ribelles JL, Perilla JE, Lebourg M. Hydrolytic degradation of PLLA/PCL microporous membranes prepared by freeze extraction. *Polym. Degrad. Stab.* 2012;97:1621–1632.
- [21] Chung C, Burdick J. Engineering cartilage tissue. *Adv. Drug. Deliver. Rev.* 2008;60:243–262.

- [22] O'Driscoll S. Current concepts review-the healing and regeneration of articular cartilage. *J. Bone. Joint Surg.* 1998;80:1795–1812.
- [23] Buckwalter J, Mankin H. Articular cartilage: degeneration and osteoarthritis, repair, regeneration, and transplantation. *AAOS Instr. Cours. Lec.* 1998;47:487–504.
- [24] Wang Y, Liu L, Guo S. Characterization of biodegradable and cytocompatible nano-hydroxyapatite/polycaprolactone porous scaffolds in degradation *in vitro*. *Polym. Degrad. Stabil.* 2010;95:207–213.
- [25] Liu A, Hong Z, Zhuang X, Chen X, Cui Y, Liu Y, Jing X. Surface modification of bioactive glass nanoparticles and the mechanical and biological properties of poly(L-lactide) composites. *Acta Biomater.* 2008;4:1005–1015.
- [26] Lee YH, Lee JH, An IG, Kim C, Lee DS, Lee YK, Nam JD. Electrospun dual-porosity structure and biodegradation morphology of Montmorillonite reinforced PLLA nanocomposite scaffolds. *Biomaterials.* 2005;26:3165–3172.
- [27] Furth M, Atala A, Van Dyke MV. Smart biomaterials design for tissue engineering and regenerative medicine. *Biomaterials.* 2007;28:5068–5073.
- [28] Tsuji H. Poly (lactide) stereocomplexes: formation, structure, properties, degradation, and applications. *Macromol. Biosci.* 2005;5:569–597.
- [29] Bendix D. Chemical synthesis of polylactide and its copolymers for medical applications. *Polym. Degrad. Stabil.* 1998;59:129–135.
- [30] Liao S, Chan C, Ramakrishna S. Stem cells and biomimetic materials strategies for tissue engineering. *Mater. Sci. Eng. C.* 2008;28:1189–1202.
- [31] Joshi M, Butola BS. Polymeric nanocomposites – polyhedral oligomeric silsesquioxanes (POSS) as hybrid nanofiller. *J. Macromol. Sci., Polym. Rev.* 2004;44:389–410.
- [32] Misra R, Alidedeoglu A, Jarrett W, Morgan S. Molecular miscibility and chain dynamics in POSS/polystyrene blends: control of POSS preferential dispersion states. *Polymer.* 2009;50:2906–2918.
- [33] Illescas S, Arostegui A, Schiraldi D, Sánchez-Soto M, Velasco J. The role of polyhedral oligomeric silsesquioxane on the thermo-mechanical properties of polyoxymethylene copolymer based nanocomposites. *J. Nanosci. Nanotechnol.* 2010;10:1349–1360.
- [34] Yen Y, Ye Y, Cheng C, Lu C, Tsai L, Huang J, Chang F. The effect of sulfonic acid groups within a polyhedral oligomeric silsesquioxane containing cross-linked proton exchange membrane. *Polymer.* 2010;51:84–91.
- [35] Verker R, Grossman E, Gouzman I, Eliaz N. TriSilanolPhenyl POSS–polyimide nanocomposites: structure–properties relationship. *Compos. Sci. Technol.* 2009;69:2178–2184.
- [36] Engstrand J, López A, Engqvist H, Persson C. Polyhedral oligomeric silsesquioxane (POSS)–poly(ethylene glycol) (PEG) hybrids as injectable biomaterials. *Biomed. Mater.* 2012;7:035013.
- [37] Wang W, Guo YI, Otaigbe JU. The synthesis, characterization and biocompatibility of poly (ester urethane)/polyhedral oligomeric silsesquioxane nanocomposites. *Polymer.* 2009;50:5749–5757.
- [38] Ayandele E, Sarkar B, Alexandridis P. Polyhedral oligomeric silsesquioxane (POSS)-containing polymer nanocomposites. *Nanomaterials.* 2012;2:445–475.
- [39] Hu Y, Grainger DW, Winn SR, Hollinger JO. Fabrication of poly(alpha-hydroxy acid) foam scaffolds using multiple solvent systems. *J. Biomed. Mater. Res A.* 2002;59:563–572.
- [40] Tomadakis MM, Robertson TJ. Pore size distribution, survival probability, and relaxation time in random and ordered arrays of fibers. *J. Chem. Phys.* 2003;119:1741–1749.
- [41] Pfaffl MW. A new mathematical model for relative quantification in real-time RT-PCR. *Nucleic Acids Res.* 2001;29:45e. Available from: <http://nar.oxfordjournals.org/content/29/9/e45.full>. doi:10.1093/nar/29.9.e45.
- [42] Andradý AL. Science and technology of polymer nanofibers. Hoboken, NJ: Wiley; 2008.
- [43] Huang ZM, Zhang YZ, Kotaki M, Ramakrishna S. A review on polymer nanofibers by electrospinning and their applications in nanocomposites. *Compos. Sci. Technol.* 2003;63:2223–2253.
- [44] Rokicki G, Piotrowska A, Kowalczyk T, Kozakiewicz J. Cyclic carbonates used in the synthesis of oligocarbonate diols involving step growth polymerization. *Polimery.* 2001;46:483–493.
- [45] Rokicki G, Kowalczyk T. Synthesis of oligocarbonate diols and their characterization by MALDI-TOF spectrometry. *Polymer.* 2000;41:9013–9031.

- [46] Rokicki G, Kowalczyk T, Glinski M. Synthesis of six-membered cyclic carbonate monomers by disproportionation of 1,3-bis(alkoxycarbonyloxy)propanes and their polymerization. *Polym. J.* 2000;32:381–390.
- [47] Rokicki G, Kowalczyk T. Cyclic carbonates and spiro-orthocarbonates – perspective monomers in the polymer chemistry of polymers. *Polimery.* 1998;43:407–415.
- [48] Ratner BD, Hoffman AS, Schoen FJ, Lemons JE. *Biomaterials science: an introduction to materials in medicine.* New York (NY): Academic Press; 1996.
- [49] Puppi D, Chiellini F, Piras AM, Chiellini E. Polymeric materials for bone and cartilage repair. *Prog. Polym. Sci.* 2010;35:403–440.
- [50] Lien SM, Ko LY, Huang TJ. Effect of pore size on ECM secretion and cell growth in gelatin scaffold for articular cartilage tissue engineering. *Acta Biomater.* 2009;5:670–679.
- [51] Yamane S, Iwasaki N, Kasahara Y, Harada K, Majima T, Monde K, Nishimura S, Minami A. Effect of pore size on in vitro cartilage formation using chitosan-based hyaluronic acid hybrid polymer fibers. *J. Biomed. Mater. Res. A.* 2007;81:586–593.
- [52] Lu H, Zhang S, Cheng L, Chen P, Zhou W, Liu J, Zhou J. Repair of articular cartilage defect with cell-loaded nano-HA/PLGA composites. *Key Eng. Mater.* 2007;330-332 II:1185–1188.
- [53] Li WJ, Laurencin CT, Caterson EJ, Tuan RS, Ko FK. Electrospun nanofibrous structure: a novel scaffold for tissue engineering. *J. Biomed. Mater. Res.* 2002;60:613–621.
- [54] Griffon DJ, Sedighi MR, Schaeffer DV, Eurell JA, Johnson AL. Chitosan scaffolds: interconnective pore size and cartilage engineering. *Acta Biomater.* 2006;2:313–320.
- [55] Kowalewski TA, Barral S, Kowalczyk T. Modeling electrospinning of nanofibers. In: Pyrz R, Rauhe JC, editors. *IUTAM symposium on modelling nanomaterials and nanosystems.* Vol. 13. Aalborg: IUTAM Bookseries, Springer Science+Business Media B.V.; 2009. p. 279–292.
- [56] Kowalczyk T, Nowicka A, Elbaum D, Kowalewski TA. Electrospinning of bovine serum albumin. Optimization and the use for production of biosensors. *Biomacromolecules.* 2008;9:2087–2090.
- [57] Fryczkowski R, Kowalczyk T. Nanofibres from polyaniline/polyhydroxybutyrate blends. *Synthetic Met.* 2009;159:2266–2268.
- [58] Bretcanu O, Misra SK, Yunos DM, Boccaccini AR, Roy I, Kowalczyk T, Blonski S, Kowalewski TA. Electrospun nanofibrous biodegradable polyester coatings on Bioglass<sup>®</sup>-based glass-ceramics for tissue engineering. *Mater. Chem. Phys.* 2009;118:420–426.
- [59] Yang F, Murugan R, Wang S, Ramakrishna S. Electrospinning of nano/micro scale poly(l-lactic acid) aligned fibers and their potential in neural tissue engineering. *Biomaterials.* 2005;26:2603–2610.
- [60] Grizzi I, Garreau H, Li S, Vert M. Hydrolytic degradation of devices based on poly(DL-lactic acid) size-dependence. *Biomaterials.* 1995;16:305–311.
- [61] Hu JCY, Athanasiou KA. Chapter 4: structure and function of articular cartilage. In: An YH, Martin KL, editors. *Handbook of histology methods for bone and cartilage.* Totowa, NJ: Humana Press; 2003. p. 73–96.
- [62] Aufderheide AC, Athanasiou KA. Mechanical stimulation toward tissue engineering of the knee meniscus. *Ann. Biomed. Eng.* 2004;32:1161–1174.
- [63] Eleswarapu SW, Responde DJ, Athanasiou KA. Tensile properties, collagen content, and crosslinks in connective tissues of the immature knee joint. *PLoS one.* 2011;6:e26178. Available from: <http://www.plosone.org/article/info%3Adoi%2F10.1371%2Fjournal.pone.0026178>. doi:10.1371/journal.pone.0026178.
- [64] Duarte R, Glazebrook MA, Castro V, Vasconcelos AC. Achilles tendinosis—a morphometrical study in a rat model. *Int. J. Clin. Exp. Pathol.* 2011;4:683–691.
- [65] Ochsner A, Ahmed W. Bone and cartilage – its structure and physical properties. In: Öchsner A, Ahmed W, editors. *Biomechanics of hard tissues.* Germany: Wiley-VCH GmbH & Co.; 2010. p. 1–75.
- [66] Minogue B, Richardson S, Zeef L, Freemont A, Hoyland J. Transcriptional profiling of bovine intervertebral disc cells: implications for identification of normal and degenerate human intervertebral disc cell phenotypes. *Arthritis. Res. Ther.* 2010;12:R22.
- [67] Martin I, Jakob M, Schäfer D, Dick W, Spagnoli G, Heberer M. Quantitative analysis of gene expression in human articular cartilage from normal and osteoarthritic joints. *Osteoarthr. Cartilage.* 2001;9:112–118.

- [68] Lin Z, Pavlos NJ, Cake MA, Wood DJ, Xu J, Zheng MH. Evidence that human cartilage and chondrocytes do not express calcitonin receptor. *Osteoarthr. Cartilage*. 2008;16:450–457.
- [69] Janjanin S, Li WJ, Morgan MT, Shanti RM, Tuan RS. Mold-shaped, nanofiber scaffold-based cartilage engineering using human mesenchymal stem cells and bioreactor. *J. Surg. Res.* 2008;149:47–56.
- [70] Toegel S, Wu SQ, Piana C, Unger FM, Wirth M, Goldring MB, Gabor F, Viernstein H. Comparison between chondroprotective effects of glucosamine, curcumin, and diacerein in IL-1 $\beta$ -stimulated C-28/I2 chondrocytes. *Osteoarthr. Cartilage*. 2008;16:1205–1212.
- [71] Jun Z, Hou HQ, Schaper A, Wendorff JH, Greiner A. Poly-L-lactide nanofibers by electrospinning-influence of solution viscosity and electrical conductivity on fiber diameter and fiber morphology. *e-Polymers*. 2003;9:1–9.
- [72] Xu X, Chen X, Liu A, Hong Z, Jing X. Electrospun poly(l-lactide)-grafted hydroxyapatite/poly(l-lactide) nanocomposite fibers. *Eur. Polym. J.* 2007;43:3187–3196.
- [73] Chen M, Patra PK, Lovett ML, Kaplan DL, Bhowmick S. Role of electrospun fibre diameter and corresponding specific surface area (SSA) on cell attachment. *J. Tissue Eng. Regen. Med.* 2009;3:269–279.
- [74] Kim K, Yu M, Zong X, Chiu J, Fang D, Seo YS, Hsiao BS, Chu B, Hadjiargyrou M. Control of degradation rate and hydrophilicity in electrospun non-woven poly(d,l-lactide) nanofiber scaffolds for biomedical applications. *Biomaterials*. 2003;24:4977–4985.
- [75] Yang Z, Best SM, Cameron RE. The influence of  $\alpha$ -tricalcium phosphate nanoparticles and microparticles on the degradation of poly(D,L-lactide-co-glycolide). *Adv. Mater.* 2009;21:3900–3904.
- [76] Boland ED, Telemeco TA, Simpson DG, Wnek GE, Bowlin GL. Utilizing acid pretreatment and electrospinning to improve biocompatibility of poly(glycolic acid) for tissue engineering. *J. Biomed. Mater. Res. B*. 2004;71:144–152.
- [77] Szentivanyi A, Chakradeo T, Zernetsch H, Glasmacher B. Electrospun cellular microenvironments: understanding controlled release and scaffold structure. *Adv. Drug Deliver. Rev.* 2011;63:209–220.